American Journal of Pathology, Vol. 156, No. 4, April 2000

Openings between Defective Endothelial Cells Explain Tumor Vessel Leakiness

Hiroya Hashizume,* Peter Baluk,* Shunichi Morikawa,* John W. McLean,* Gavin Thurston,* Sylvie Roberge,† Rakesh K. Jain,† and Donald M. McDonald*

From the Cardiovascular Research Institute and Department of Anatomy, University of California, San Francisco, California; and the Edwin L. Steele Laboratory,† Department of Radiation Oncology, Massachusetts General Hospital and Harvard Medical School, Boston, Massachusetts*

Leakiness of blood vessels in tumors may contribute to disease progression and is key to certain forms of cancer therapy, but the structural basis of the leakiness is unclear. We sought to determine whether endothelial gaps or transcellular holes, similar to those found in leaky vessels in inflammation, could explain the leakiness of tumor vessels. Blood vessels in MCa-IV mouse mammary carcinomas, which are known to be unusually leaky (functional pore size 1.2–2 μm), were compared to vessels in three less leaky tumors and normal mammary glands. Vessels were identified by their binding of intravascularly injected fluorescent cationic liposomes and *Lycopersicon esculentum* lectin and by CD31 (PECAM) immunoreactivity. The luminal surface of vessels in all four tumors had a defective endothelial monolayer as revealed by scanning electron microscopy. In MCa-IV tumors, 14% of the vessel surface was lined by poorly connected, overlapping cells. The most superficial lining cells, like endothelial cells, had CD31 immunoreactivity and fenestrae with diaphragms, but they had a branched phenotype with cytoplasmic projections as long as 50 μm. Some branched cells were separated by intercellular openings (mean diameter 1.7 μm; range, 0.3–4.7 μm). Transcellular holes (mean diameter 0.6 μm) were also present but were only 8% as numerous as intercellular openings. Some CD31-positive cells protruded into the vessel lumen; others sprouted into perivascular tumor tissue. Tumors in RIP-Tag2 mice had, in addition, tumor cell-lined lakes of extravasated erythrocytes. We conclude that some tumor vessels have a defective cellular lining composed of disorganized, loosely connected, branched, overlapping or sprouting endothelial cells. Openings between these cells contribute to tumor vessel leakiness and may permit access of macromolecular therapeutic agents to tumor cells. *(Am J Pathol 2000, 156:1363–1380)*

Much excitement has been generated by the idea of attacking and destroying tumors by exploiting abnormalities of their blood vessels. Such abnormalities could provide the opportunity to destroy tumor vessels without destroying the microvasculature of normal tissues. Tumor vessels differ from normal vessels in multiple ways. Their structural irregularity, heterogeneity, and leakiness can be regarded as bizarre hallmarks of a propensity to break all the rules of normal blood vessel construction. Most tumor vessels have an irregular diameter and abnormal branching pattern, and they do not fit well into the usual classification of arterioles, capillaries, or venules.[1–4] Vessels with a normal smooth muscle coat are infrequent. Even large-caliber vessels have thin walls. In addition, some vessels have an incomplete basement membrane and an abnormal pericyte coat.[5–8] Other abnormalities include unusually avid binding and uptake of cationic liposomes, and expression of integrins, growth factors, and receptors that differ from those of normal vessels.[9–14]

Of particular functional importance, tumor vessels are unusually leaky.[15–20] Vessel leakiness correlates with histological grade and malignant potential of tumors.[21] Furthermore, the leakiness of tumor vessels can result in extravasation of plasma proteins and even erythrocytes and may facilitate the traffic of tumor cells into the bloodstream and the formation of metastases.[19,22–24] Understanding the basis for this abnormal permeability is key to the effective delivery of chemotherapeutic agents to tumor cells and to monitoring the efficacy of antiangiogenic therapy.

Evidence for increased endothelial permeability of tumor vessels has come from many sources. Extravasation of soluble tracers such as radioisotopes, albumin, fibrinogen, dextran, horseradish peroxidase, Lissamine green, and ferritin has been demonstrated in experimental tumors.[16,25–28] Studies of the extravasation of blood-borne particulates such as colloidal carbon and sterically sta-

Supported in part by National Institutes of Health grants HL-24136 and HL-59157 from the National Heart, Lung and Blood Institute (to D. M.) and R35-CA-56591 from the National Cancer Institute (to R. J.) and by a grant from MBT Munich Biotechnology GmbH in Munich, Germany (to D. M.). D. M., J. M., and G. T. have equity positions in Munich Biotechnology.

Accepted for publication January 6, 2000.

H. H.'s present address: Department of Anatomy, Niigata University School of Medicine, Asahimachi-dori 1, Niigata 951-8510, Japan.

Address reprint requests to Donald M. McDonald, M.D., Ph.D., Cardiovascular Research Institute, University of California, 513 Parnassus Avenue, San Francisco, CA 94143-0130. E-mail: dmcd@itsa.ucsf.edu.

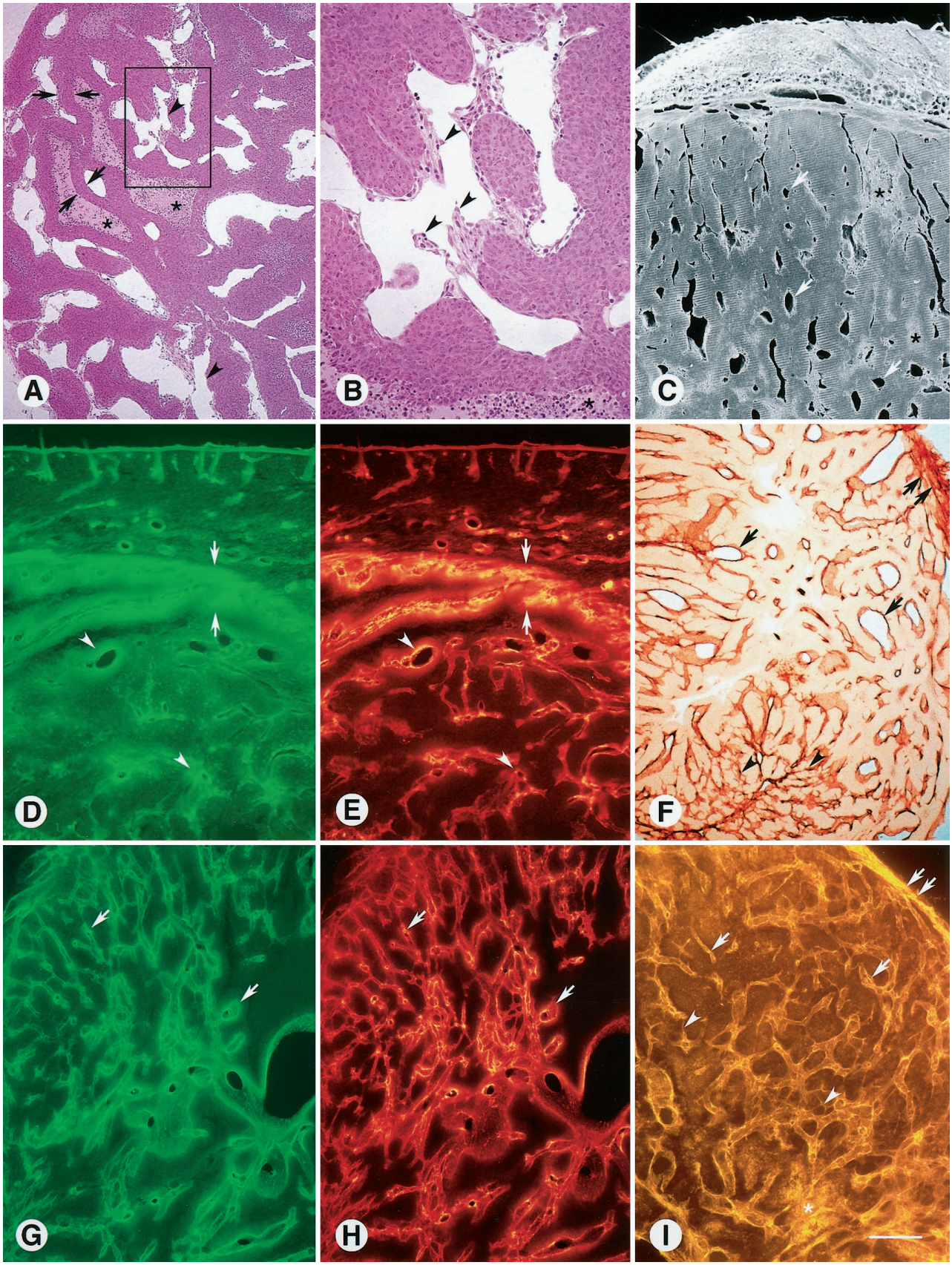
A
B
C
D
E
F
G
H
I

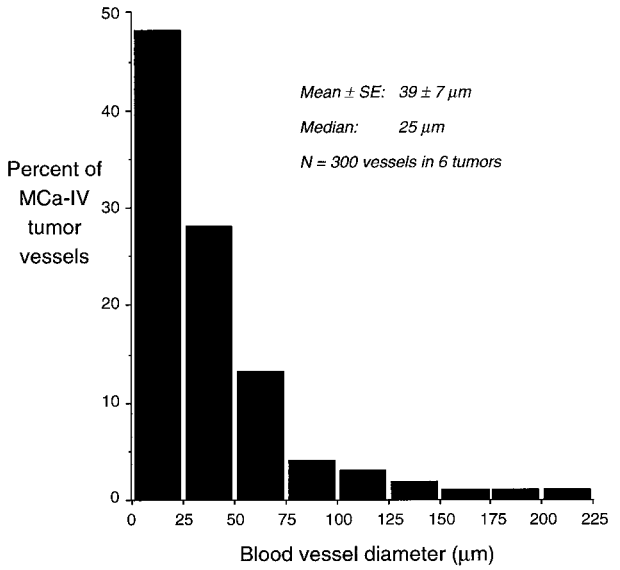

Figure 2. Bar graph showing size distribution of vessels in MCa-IV tumors. Diameters of 50 blood vessel profiles were measured in hematoxylin-and-eosin-stained, 2-μm methacrylate sections of each of 6 tumors.

bilized (stealth) liposomes has revealed functional pore sizes as large as 2 μm in tumor vessels.[29–31] Scanning electron microscopy (EM) has shown the extravasation of intravenously (i.v.) injected plastic casting media in some tumors.[3,32] The leakiness of tumor vessels has also been documented by magnetic resonance imaging of i.v. injected contrast media.[33,34] Intratumoral hemorrhage is a manifestation of vessel leakiness that can range from scattered extravasated erythrocytes to blood lakes (also called hemorrhagic lakes or vascular lakes), which are large collections of erythrocytes surrounded by tumor cells.[22,35–38] Alternatively, blood lakes could be abnormal vascular channels connected to the bloodstream.[39,40]

Vessel leakiness in tumors has been attributed to highly active angiogenesis and microvascular remodeling, but the structural basis and mechanism of the leakage are unclear. Intercellular gaps, transendothelial holes, vesiculo-vacuolar organelles, and endothelial fenestrae are all reportedly present in the endothelium of tumor vessels.[19,41] However, the relative frequency and contribution of these to vessel leakiness have not been studied extensively. By comparison, the mechanism of vessel leakiness in inflammation is much better characterized. Most studies point to the involvement of transiently open intercellular gaps in leakage from inflamed vessels.[42,43] Under some conditions transcellular holes may also play a role.[44]

The purpose of the present study was to identify structural abnormalities in the endothelium of tumor blood vessels that could explain their leakiness. In particular, we sought to determine whether the vessels have intercellular gaps or transcellular holes similar to those found in leaky vessels of inflamed tissues. We also determined whether blood lakes in tumors are collections of erythrocytes that have extravasated from leaky blood vessels or abnormal vascular channels connected to the bloodstream.

We reasoned that structural abnormalities should be most easily detected in tumors with very leaky vessels. Therefore, our strategy was to focus on a tumor, MCa-IV mouse mammary carcinoma, that is known to have blood vessels on the high end of the range of leakiness for tumors, as evidenced by a functional pore size of 1200 to 2000 nm.[31] Less leaky Shionogi mammary tumors (pore size 200–380 nm), LS174T colon carcinomas (pore size 400–600 nm), and normal mouse mammary glands were used for comparison. In addition, insulinomas in RIP-Tag2 transgenic mice, which have a bloody appearance, were used to examine the nature of blood lakes in tumors.[45,46] After tissues were fixed by vascular perfusion, we used CD31 immunohistochemistry, binding of intravascular lectins, uptake of fluorescent cationic liposomes, and vascular labeling with the particulate tracer Monastral blue to confirm the identity of blood vessels and to minimize the chance of misinterpreting abnormal vessel-like spaces in tumors. This approach also made it possible to distinguish between intravascular erythrocytes and extravascular erythrocytes. Then the luminal surface of vessels exposed in Vibratome sections was examined by scanning EM to identify intercellular gaps, transcellular holes, or other potential sites of leakage across the endothelium. The scanning EM observations were confirmed by transmission EM.

Materials and Methods

Animals and Tumors

Two-millimeter cubes of MCa-IV mouse mammary carcinomas were implanted under the dorsal skin of male C3H mice (25–30 g) in the animal facility of University of California San Francisco or the Edwin L. Steele Laboratory, Department of Radiation Oncology, Massachusetts General Hospital, as previously described.[31] The tumors grew to a diameter of 8 to 12 mm over 14 to 20 days.[31] For comparison, Shionogi tumors (mouse testosterone-dependent male mammary carcinomas) and LS174T hu-

Figure 1. Diverse size and morphology of blood vessels in MCa-IV tumors. **A:** Hematoxylin-and-eosin-stained 2-μm methacrylate section showing irregularly shaped blood vessels (**arrowheads**) emptied of blood by vascular perfusion and surrounded by sleeves of tumor cells (**arrows**) interspersed by necrotic tissue (*). Region in box is shown at higher magnification in **B**. **B:** Irregular luminal lining layer (**arrowheads**) of vessel surrounded by tumor cells. Necrotic tissue is present at the bottom (*). **C:** Scanning EM view of 100-μm Vibratome section of a subcutaneous MCa-IV tumor with skin at the top. Blood vessels appear as black holes (**arrows**). Necrotic tissue is pale (*). **D:** FITC-labeled *L. esculentum* lectin (green) marks blood vessels in 100-μm section of tumor with overlying skin at the top. Extravasation of lectin, which makes vessel borders appear fuzzy (**arrowheads**), is most conspicuous in the tumor's highly vascular capsule (**arrows**). **E:** Fluorescent cationic liposomes (red) mark the same blood vessels as those labeled with lectin in **D**. Vessel borders (**arrowheads**) are more clearly defined than with the lectin because of the lack of extravasation. Capsule, **arrows**. **F:** Brightfield image showing CD31 immunoreactivity in 100-μm section of tumor. Both blood vessels (**arrows**) and tiny sprouts (**arrowheads**) have CD31 immunoreactivity. Densely vascular capsule (**double arrows**). **G** and **H:** Region of tumor with a wide range of vessel size (**arrows**) shown by green lectin colocalized with red cationic liposomes. **I:** Tumor with CD31-immunofluorescent blood vessels (**arrows**), tiny sprouts (**arrowheads**), and densely vascular capsule (**double arrows**). Necrotic region (*) has nonspecific fluorescence. Scale bar in **I** applies to all figures; bar length represents 300 μm in **A**, **D**, **E**, and **G–I**; 80 μm in **B**; and 400 μm in **C** and **F**.

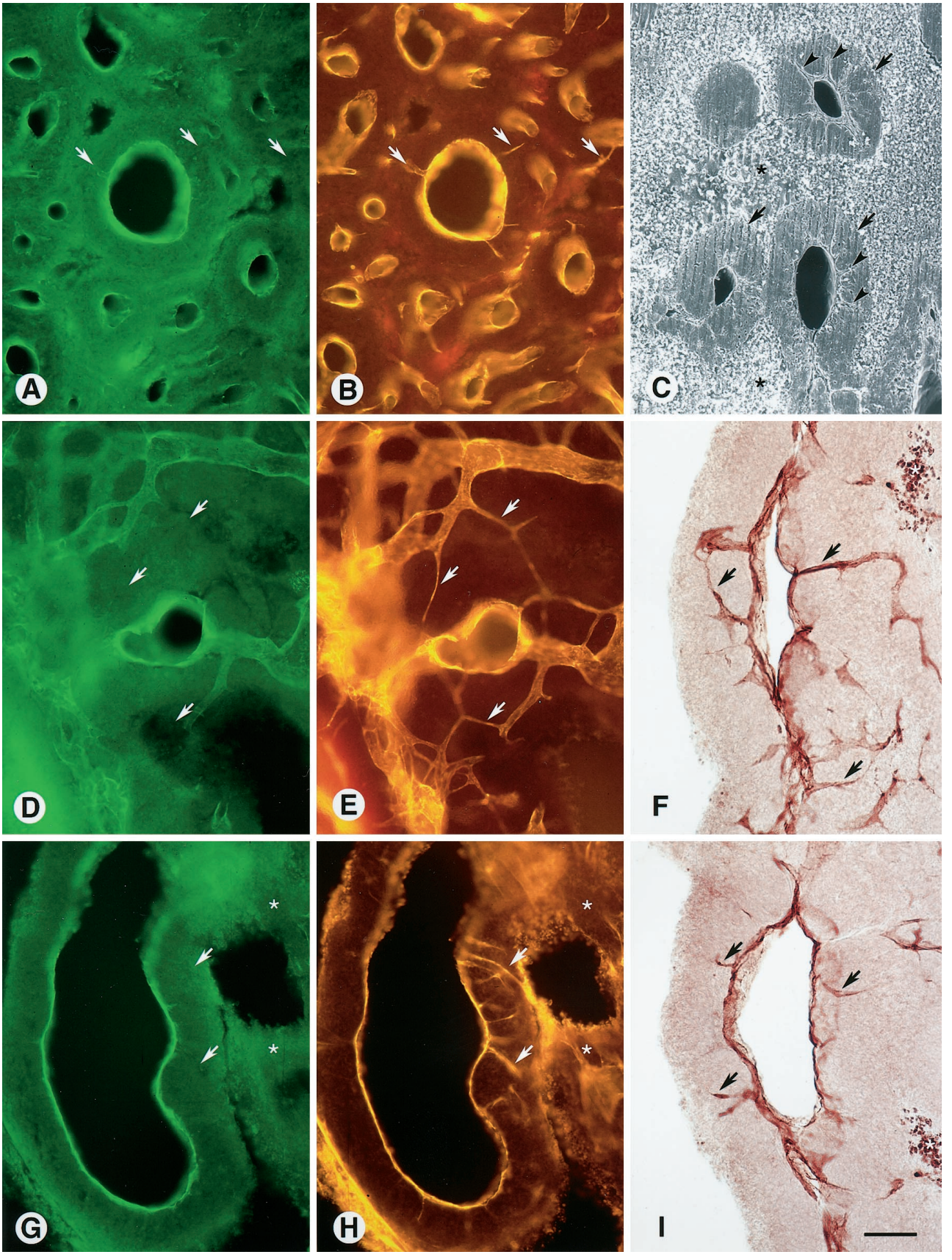
A
B
C
D
E
F
G
H
I

man colon adenocarcinomas were grown subcutaneously to a diameter of about 8 mm over 14 to 20 days in male *SCID* mice.[31] Spontaneous pancreatic islet cell tumors were studied in RIP-Tag2 transgenic mice at 8 to 14 weeks of age.[47] Blood vessels were also examined in normal mammary glands of C3H mice. Mice were anesthetized with ketamine (87 mg/kg) plus xylazine (13 mg/kg) injected together intramuscularly. The chest was opened rapidly, and the vasculature was perfused for 2 minutes at a pressure of 120–140 mmHg with fixative from a cannula (blunt 18 gauge needle) inserted into the ascending aorta via an incision in the left ventricle. The cannula was immediately clamped in place (time from heart incision to perfusion <15 seconds). The composition of the fixative varied with the purpose of the experiment (see below). The fixative was not preceded by a buffer or saline rinse. The right atrium was incised to create a route for the fixative to exit. With this approach, the vasculature was washed free of blood and preserved in an open state; the only blood remaining in tumors was extravasated erythrocytes. All experimental procedures were approved by the Committees on Animal Research of University of California San Francisco and the Massachusetts General Hospital.

Scanning Electron Microscopy

For scanning EM, tissues were fixed by vascular perfusion of 0.5% glutaraldehyde and 1% paraformaldehyde in 0.075 mol/L sodium cacodylate buffer, pH 7.4. Tumors were removed, immersed in 2.5% glutaraldehyde in cacodylate buffer for a minimum of 2 hours, and embedded in 10% agarose. The luminal surface of blood vessels in tumors was exposed by cutting Vibratome sections 100 μm in thickness. The sections were rinsed with cacodylate buffer, immersed in cacodylate buffered 2% tannic acid for 24 hours, rinsed, and then immersed in 2% OsO_4 in 0.1 mol/L cacodylate buffer for 2 hours at 4°C.[48] After dehydration with ethanol, sections were infiltrated with 100% *t*-butanol and freeze-dried under vacuum. Sections were sputter-coated with a 4- to 16-nm-thick layer of gold-palladium alloy. The luminal surface of vessels was photographed with a JEOL JSM-840A or Hitachi S-2380N scanning electron microscope.

Brightfield and Fluorescence Microscopy

For routine histology, tissues were fixed by vascular perfusion of 0.5% glutaraldehyde and 1% paraformaldehyde in phosphate-buffered saline (PBS), embedded in glycol methacrylate resin (JB-4, Polysciences, Warrington, PA), sectioned at 2 μm thickness, and stained with hematoxylin and eosin. Specimens were examined with a Zeiss Axiophot microscope equipped for brightfield, differential interference contrast, and epifluorescence.

Tumor vasculature was made visible by labeling with biotin- or fluorescein isothiocyanate (FITC)-labeled *Lycopersicon esculentum* lectin (100 μg in 100 μl 0.9% NaCl, Vector Laboratories, Burlingame, CA) injected into the femoral vein of anesthetized mice, and 2 minutes later fixative containing 0.5% glutaraldehyde and 1% paraformaldehyde in PBS was perfused through the vasculature. Tumors were embedded in 10% agarose and cut with a Vibratome or cryostat (100 μm thickness). Biotin-labeled lectin was visualized by incubation overnight with avidin-biotin peroxidase complex (ABC; Vector Laboratories) diluted 1:250 in phosphate-buffered saline containing 0.3% Triton-X 100 (PBS/Triton) followed by diaminobenzidine (DAB; Sigma Chemical Company, St. Louis, MO), dehydration, and mounting in Permount (Fisher Scientific, San Francisco, CA).[49] The detergent permeabilized tissues, increasing the penetration of reagents into the 100-μm sections. FITC-labeled lectin in sections mounted in Vectashield (Vector) was visualized by fluorescence microscopy.

Tumor blood vessels were also visualized by their uptake of fluorescent cationic liposomes, which have a high affinity for endothelial cells in tumors and other sites of angiogenesis.[12,50] Cationic liposomes approximately 50 nm in diameter, consisting of 55% 1,2-dioleoyl-3-trimethylammonium-propane (DOTAP), 44% cholesterol, and 1% rhodamine-DHPE (1,2-dihexadecanoyl-*sn*-glycero-3-phosphoethanolamine) were prepared by sonication and suspended in 5% dextrose.[50] Lipids were purchased from Avanti Polar Lipids (Alabaster, AL). The liposome suspension (1440 nmol total lipid in 150 μl of 5% dextrose) was injected into a femoral vein 20 minutes before vascular perfusion of fixative (0.5% glutaraldehyde and 1% paraformaldehyde in PBS). Some mice received i.v. injections of both liposomes and FITC-labeled lectin to assess colocalization of the two markers. Vibratome or cryostat sections were cut, mounted, and viewed by fluorescence microscopy.

The question of whether blood lakes in tumors of RIP-Tag2 mice were connected to the vasculature was addressed by labeling blood vessels with fluorescent lectin or cationic liposomes injected i.v. as described above. Alternatively, the particulate tracer Monastral blue (1 μl/g body weight of 3% suspension of copper phthalocyanine blue pigment BW-431-P, Chemicals and Pigments Department, E. I. duPont deNemours and Company, Wilmington, DE) was injected into a femoral vein of anesthe-

Figure 3. Blood vessels in MCa-IV tumors marked by green fluorescent lectin staining (**A, D,** and **G**) or CD31 immunoreactivity viewed by Cy3 fluorescence (**B, E,** and **H**) and ABC-DAB histochemistry (**F** and **I**) in 100-μm Vibratome sections. Necrotic tissue (*). **A** and **B:** Like the lectin, CD31 immunoreactivity defines the luminal surface of tumor vessels, but, unlike the lectin, it is also present on sprouts (**arrows**) radiating from the vessel lining into the tumor. **C:** Scanning EM showing lumenless sprouts (**arrowheads**), similar to those in **A** and **B**, radiating into sleeves of tumor tissue (**arrows**). Necrotic tissue surrounds the tumor sleeves. **D** and **E:** Tiny sprouts (**arrows**), which apparently have no lumen because they have CD31 immunoreactivity but no lectin staining, are about 1 μm in diameter and interconnect tumor vessels. **F:** CD31-immunoreactive sprouts (**arrows**), made visible by ABC-DAB histochemistry, extend from the vessel surface into the tumor. **G** and **H:** Lumenless CD31-immunoreactive sprouts (**arrows**) without lectin staining penetrate the sleeve of tumor tissue. **I:** CD31-immunoreactive sprouts (**arrows**) radiate from the perimeter of a vessel into the tumor. Scale bar in **I** applies to all figures; bar length represents 150 μm in **A, B, D, E, G,** and **H**; 100 μm in **C**; 75 μm in **F** and **I**.

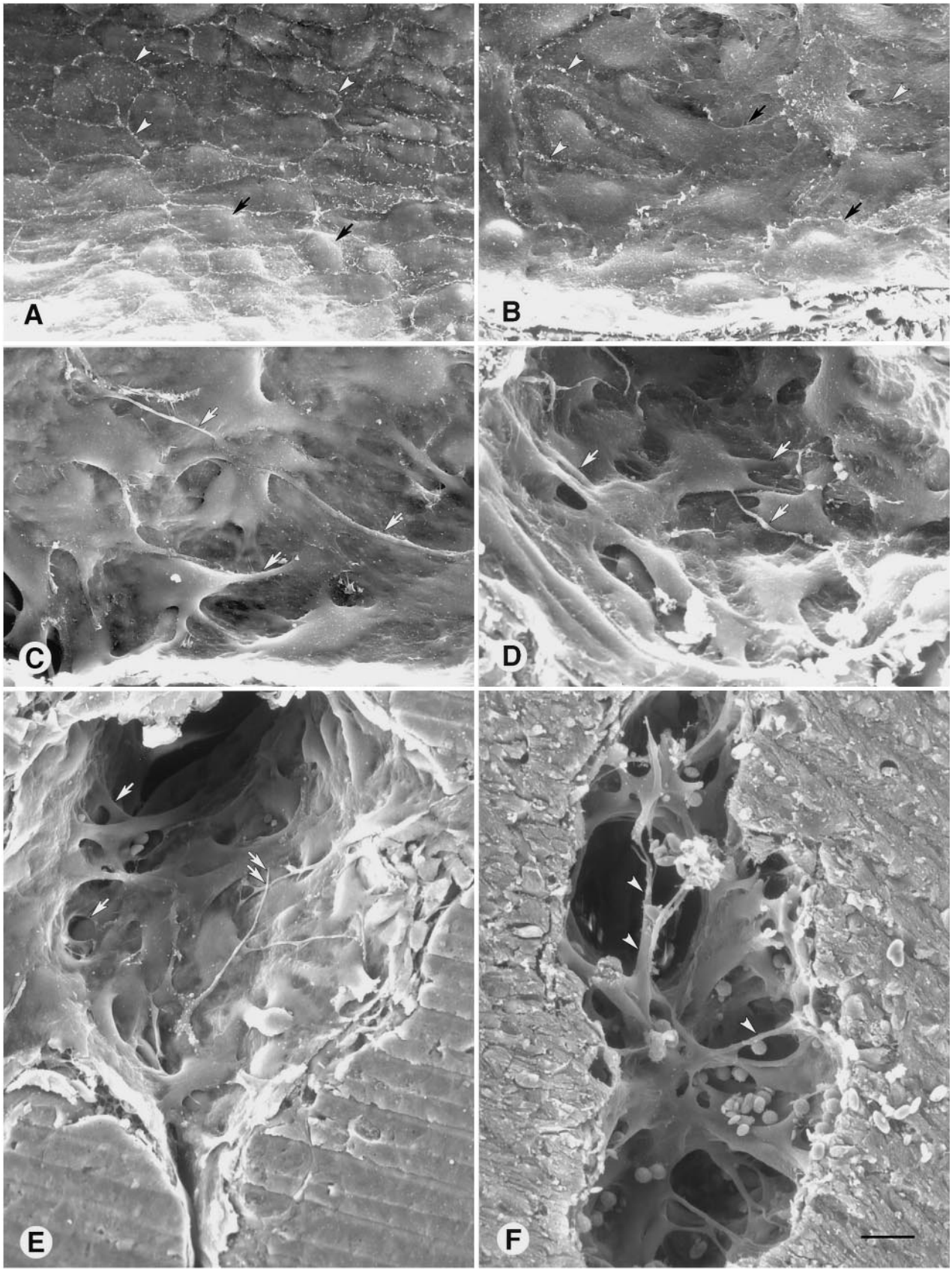
A
B
C
D
E
F

tized mice, and 10 or 20 minutes later fixative (0.5% glutaraldehyde and 1% paraformaldehyde in PBS) was perfused through the vasculature. The pancreas and its tumors were removed as a block, and sites of Monastral blue labeling were localized by brightfield microscopy in whole mounts mounted in Permount.

Endothelial cells were localized by CD31 (PECAM) immunohistochemistry in tumors fixed by vascular perfusion of 4% paraformaldehyde in PBS and embedded in 10% agarose (Sigma) or infiltrated overnight with 30% sucrose and frozen. Sections 100 μm in thickness, cut with a Vibratome or cryostat, were incubated at room temperature for 12 to 15 hours in rat anti-mouse CD31 monoclonal antibody (Pharmingen, San Diego, CA) diluted 1:500 followed by 6 hours in biotin- or Cy3-labeled donkey secondary anti-rat IgG antibody (Jackson ImmunoResearch, West Grove, PA) diluted 1:200 in PBS/Triton. Sections were then processed and viewed as for lectin staining.

Transmission EM

Tumors were fixed by vascular perfusion of aldehyde fixative as for scanning EM. Specimens measuring approximately 1 × 3 mm were cut from 100-μm Vibratome sections, treated with OsO_4 and uranyl acetate, dehydrated, and embedded in epoxy resin.[51] Sections 0.5 μm in thickness were stained with toluidine blue for light microscopy, and sections 50–100 nm in thickness were stained with lead citrate and examined with a Zeiss EM-10 electron microscope.

Morphometry and Statistical Analysis

Diameters of 300 blood vessels in six MCa-IV tumors were measured in video images of methacrylate sections with a digitizing tablet interfaced with a computer.[51] Approximately 700 cells lining blood vessels of MCa-IV tumors in 5 mice were photographed by scanning EM at both low and high magnifications as needed for different measurements. The proportions of branched and unbranched lining cells were determined in 20 vessels having a total visible surface area of 220,000 μm^2 (magnification, 500 to 1000×). The luminal surface area and perimeter of a sample of 25 unbranched cells and 25 branched cells in 35 vessels were measured using a digitizing tablet (magnification, 2000 to 5000×). The shape index of cells was calculated from their area A and perimeter P by the equation $4\pi \times A/P^2$, where the shape index of a circle is 1. The shape index decreases as the profile becomes more elongated or irregular. The area and perimeter of 100 intercellular openings between the 700 lining cells (magnification, 2000 to 10,000×) were measured, as were the 8 transcellular holes identified along with the openings. Intercellular openings that exposed the plasma membrane of an underlying cell were excluded because they were assumed not to be pathways for extravasation. Area measurements were used to calculate the total amount of luminal surface examined (291,000 μm^2) and the combined areas of the openings (292 μm^2) and holes (2.3 μm^2). The diameter of intercellular openings and transcellular holes was estimated from their areas (2 * SQRT(A/π)) or perimeters ($P/2\pi$), with the assumption that they were roughly circular. Values are presented as means ± SE. The significance of differences between means was assessed by Student's t-test.

Results

Identification of Blood Vessels in MCa-IV Tumors

Several different methods of identification were used to verify that the blood vessel-like structures in MCa-IV tumors were not artifactual spaces, cysts, collections of extravasated erythrocytes, or other abnormalities. By all methods, the blood vessels were found to be emptied of blood and preserved in an open state by the vascular perfusion of fixative. In hematoxylin-and-eosin-stained sections of MCa-IV tumors, blood vessels were abundant, thin-walled, and surrounded by 100-μm thick sleeves of tumor cells interspersed by regions of necrosis (Figure 1A). The vessels were variable in size (diameter 39 ± 7 μm, range 8–220 μm, 300 vessels in 6 tumors). Larger vessels were conspicuous and easily identified by their size and their thin but distinct wall (Figure 1B), but small vessels predominated, with 48% being 25 μm or less in diameter (Figure 2). Most large vessels were separated from tumor cells by a perivascular space as wide as 20 μm containing stromal cells and extracellular matrix, yet some were much closer to tumor cells (Figure 1B). Collections of extravasated erythrocytes were rare in MCa-IV tumors but were common in islet cell tumors in RIP-Tag2 mice (see below). MCa-IV tumors were surrounded by a capsule. Most of these features, including the blood vessels, perivascular sleeves of tumor cells, regions of necrosis, and capsule, were also visible by scanning EM (Figure 1C).

Intravenous green fluorescent *L. esculentum* lectin, which binds to the luminal surface of blood vessels, and red fluorescent cationic liposomes, which avidly bind to and are taken up by the vessel lining cells of tumor vessels,[12,50] clearly defined the vasculature of MCa-IV

Figure 4. Scanning EM view of luminal surface of normal endothelial cells in mammary gland compared to a range of abnormalities in vessel lining cells in MCa-IV tumors. **A:** Endothelial cells in this normal venule have a relatively uniform size and shape and are flat except for the region of the nucleus (**arrows**). Cells form a monolayer, and cell borders (**arrowheads**) have little overlap. **B:** Unbranched endothelial cells in a tumor vessel are irregularly shaped and overlap one another (**arrows**). Some cell borders are clearly visible (**arrowheads**); others are not. **C** and **D:** More severely deformed, branched endothelial cells in tumor vessels. These cells overlap one another, are abnormally thick, have multiple cell projections (**arrows**), and do not have normal connections with other cells. **E:** Luminal surface of a tumor vessel showing branched lining cells with extensive cellular overlap, bridges and tunnels (**arrows**), and cellular projections as long as 50 μm (**double arrows**). **F:** Abnormal lining cells that partition (**arrowheads**) the lumen of a tumor vessel. Scale bar in **F** applies to all figures; bar length represents 10 μm in **A–D** and 15 μm in **E** and **F**.

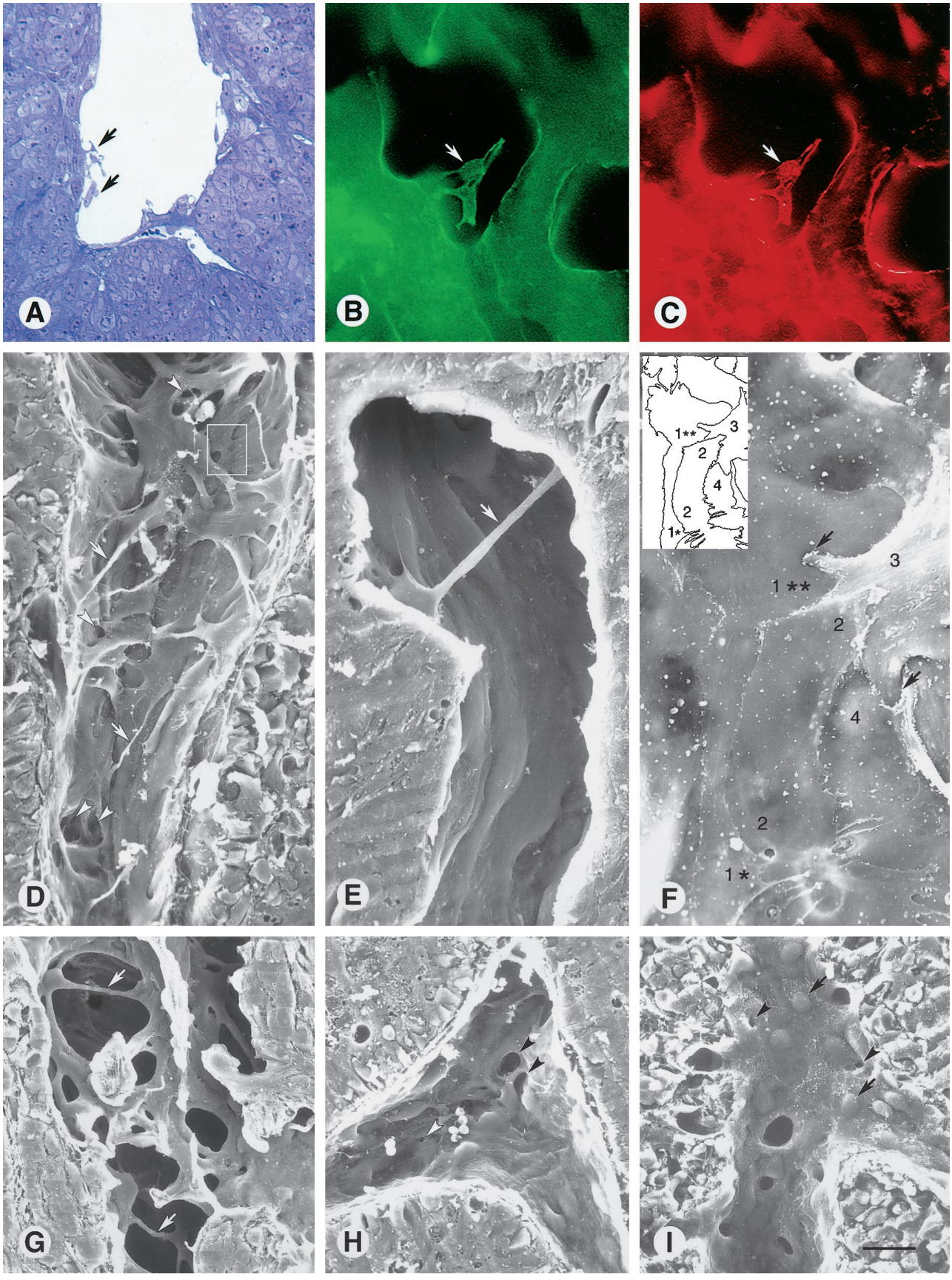
A
B
C
D
E
F
1**
3
2
4
2
1*
1 **
3
2
4
2
1 *
G
H
I

tumors (Figure 1, D and E). (The term "vessel lining cells" is used instead of "endothelial cells" to describe the cells in contact with blood in tumor vessels because of the possibility that some of these cells may not be endothelial cells.) Green lectin and red liposomes were colocalized in the abundant small vessels in the capsule at the tumor surface as well as on vessels of all sizes within the tumor (Figure 1, D and E). (We do not categorize tumor vessels as arterioles, capillaries, or venules because the vessels lack the structural characteristics of normal vasculature that make these terms meaningful.) The labeled vessels had an irregular shape and widely variable diameter and branching pattern (Figure 1, G and H), which was quite unlike the uniform, smooth, cylindrical contour of the normal microvasculature. Extravasation of the lectin blurred the labeling of some vessels (Figure 1, D and G) and resulted in green fluorescence of scattered regions of extravascular cells. No evidence of liposome extravasation was detected. In addition to the red coating of the lining cells, some liposome fluorescence was punctate, consistent with an endosomal location.

The pattern of CD31 immunoreactivity in MCa-IV tumors (Figure 1F) was more complex and extensive than the vessel pattern shown by lectin staining or cationic liposome binding (Figure 1, D and E). Although the overall arrangement of vessels was similar, more structures had CD31 immunoreactivity than were stained by the other methods (Figure 1I). In particular, thin CD31-immunoreactive sprout-like filaments, without a lumen detectable by lectin staining (Figure 3A), radiated from some vessel walls into the perivascular sleeves of tumor (Figure 3B). Similar sprouts were evident by scanning EM, and again no lumen was visible (Figure 3C). Many of these traversed the 100-μm thickness of the sleeves of tumor tissue, and some contacted other vessels (Figure 3, D and E). CD31 immunoreactivity colocalized with lectin staining on the vessel lining but not on the sprouts that radiated from vessel walls into the tumor (Figure 3, G and H), indicating that these sprouts did not have a lumen connected to the blood circulation. CD31-immunoreactive sprouts were particularly conspicuous when visualized by DAB staining (Figure 1, F and I).

Vessel Lining Cells

Blood vessels of normal mammary glands examined by scanning EM were lined by flat endothelial cells that were closely apposed to one another, had a smooth contour, and were demarcated by slightly raised margins (Figure 4A). The endothelial cells formed a continuous, uniform monolayer, as has been described in the microcirculation of other organs.[48,51] The longest cytoplasmic projections of endothelial cells measured less than 1 μm.

Scanning EM observations of MCa-IV tumors revealed that most of the lining cells of blood vessels of the type labeled by cationic liposome binding and lectin staining were morphologically abnormal. The shape of the lining cells ranged from somewhat irregular to bizarre (Figure 4, B–D).

The vessel lining cells in MCa-IV tumors probably represented a continuous spectrum of shapes but tended to fall into two groups, designated unbranched cells and branched cells, based on whether they had long cytoplasmic projections. An average of 86 ± 2% of the vessel surface was covered by unbranched cells (20 vessels in 5 MCa-IV tumors). These cells differed from endothelial cells in vessels of normal mammary glands because of their variable size and irregular shape (Figure 4, A and B). Some of the cells had a protruding nucleus, ruffled margins, prominent cytoskeleton, or short stubby processes (Figure 4B).

The remaining 14 ± 2% of the luminal surface of vessels in MCa-IV tumors was covered by branched cells (Figure 4, C and D). These cells typically were multipolar, and some had projections as long as 50 μm (Figure 4E). The cells were conspicuous because of their highly irregular shape, abnormal thickness, partial detachment, and long cytoplasmic projections that overlapped other lining cells (Figure 4E) or bridged the vessel lumen (Figure 4F). Cells corresponding to the branched cells were also evident by light microscopy (Figure 5A). Some branched cells that were stained with lectin and CD31 immunoreactivity extended well into the vessel lumen (Figure 5, B and C).

Consistent with their irregular shape, branched cells had a lower shape index than the unbranched cells (0.23 ± 0.02 *vs.* 0.42 ± 0.03; $p < 0.01$, 25 cells of each type sampled from 35 vessels in 5 tumors). Branched cells also tended to be smaller than the unbranched cells, but the difference was not statistically significant (luminal surface area 295 ± 49 μm^2 *vs.* 430 ± 90 μm^2; same sample of 25 cells of each type).

Defective Endothelial Monolayer

Branched cells did not form an intact monolayer, as judged by scanning EM. Instead, the cells formed two, three, or perhaps more incomplete layers in which the cells next to the lumen covered underlying cells, and cell projections extended between the layers (Figure 4, E and

Figure 5. A–F: Blood vessel lining cells (**arrows**) that protrude into the lumen of vessels in MCa-IV tumors. Vasculature emptied of blood by perfusion of fixative. **A:** Protruding cells in a large, thin-walled vessel in a toluidine blue-stained 0.5-μm epoxy section photographed at low magnification. **B** and **C:** Protruding cells (**arrow**) in a tumor vessel (black lumen) labeled with FITC-lectin (green) and rhodamine-cationic liposomes (red). **D:** Scanning EM view of a vessel with lining cells that protrude into the lumen as in **A–C**. Extensive cellular overlap, numerous cytoplasmic projections (**arrows**), and openings between cells (**arrowheads**) are present. White box marks region shown at higher magnification in Figure 7, B and C. **E:** Lining cell with a thread-like process that spans the vessel lumen. **F:** Overlapping lining cells in tumor vessel. One region (*) of the cell marked 1 is located above cell 2, which in turn is superficial to cells 3 and 4, but another region (**) of cell 1 is beneath cells 2 and 3. Projections from cell 3 appear to penetrate cells 1 and 4 (**arrows**). **Inset** shows outline of endothelial cell borders. **G:** Lining cells with numerous transluminal cytoplasmic processes (**arrows**) in a blood vessel of a Shionogi male mammary carcinoma. **H:** Openings (**arrowheads**) and other defects in the vessel lining of a LS174T human colon carcinoma grown in a SCID mouse. **I:** Openings (**arrowheads**) and other defects in the vessel lining of an islet cell tumor in a transgenic RIP-Tag2 mouse. Scale bar in **I** applies to all figures; bar length represents 25 μm in **A** and **G–I**; 50 μm in **B** and **C**; 20 μm in **D**; 10 μm in **E**; 5 μm in **F**.

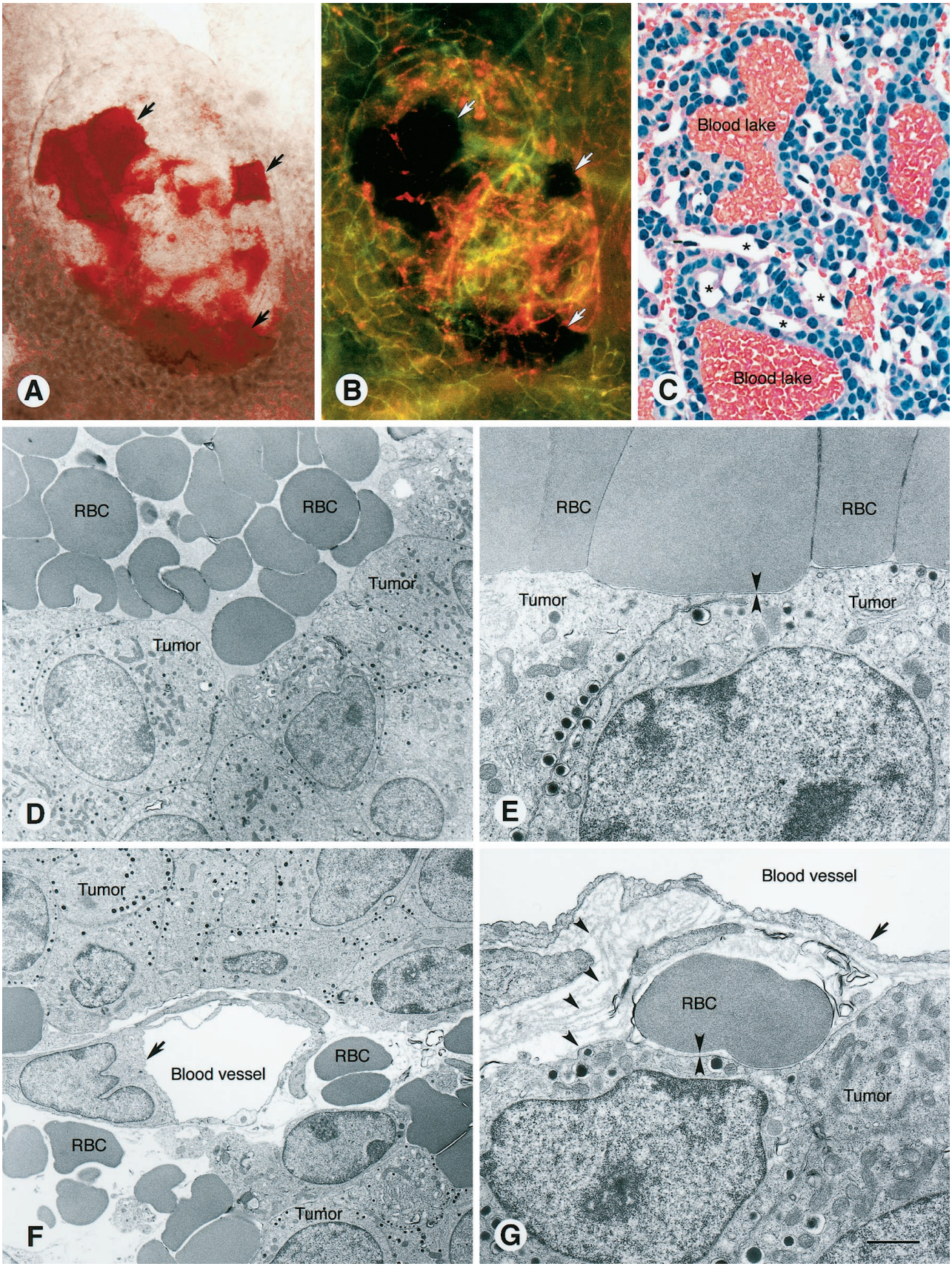
A
B
C
Blood lake
Blood lake
D
RBC
RBC
Tumor
Tumor
E
RBC
RBC
Tumor
Tumor
F
Tumor
Blood vessel
RBC
RBC
Tumor
G
Blood vessel
RBC
Tumor

F). Projections of some branched cells spanned the luminal surface of one or more neighboring cells (Figure 5D) or bridged the vessel lumen (Figure 5E). Other cell projections penetrated between or even through adjacent cells (Figure 5F). Regions of branched cells between the projections formed tunnels of various size, length, and complexity where they arched over other lining cells (Figures 4E, 4F, and 5D). The arches created intercellular openings in the vessel wall (see below).

Defects in the endothelial monolayer and lining cells with bizarre branched shapes were also found by scanning EM in vessels of Shionogi testosterone-dependent male mouse mammary carcinomas, LS174T human colon adenocarcinomas, and spontaneous pancreatic islet cell tumors in RIP-Tag2 mice. Some lining cells formed arches, transluminal processes, or multiple layers (Figure 5, G–I). However, the abnormalities were less severe than those in MCa-IV tumors.

Tumors in RIP-Tag2 mice not only had vessels with a defective lining but also contained extravasated erythrocytes that gave them a bloody appearance even after vascular perfusion of fixative (Figure 6A). Some of the extravasated erythrocytes were located in discrete blood lakes (Figure 6A). Unlike blood vessels, blood lakes were not labeled by fluorescent lectin or cationic liposomes injected into the vasculature (Figure 6B). Similarly, Monastral blue injected i.v. was not found within the lumen or wall of blood lakes but did label some vessels at the tumor surface. Thus, there was no evidence that the blood lakes were directly connected to the bloodstream. Although the lakes resembled large, sack-like blood vessels or sinusoids by light microscopy (Figure 6C), it was obvious by transmission EM that they were lined by tumor cells, not endothelial cells (Figure 6D). Indeed, some erythrocytes were immediately adjacent to tumor cells (Figure 6E). The extravascular location of erythrocytes in RIP-Tag2 tumors was unambiguous near blood vessels where the vessel lumen and lining cells were visible (Figure 6, F and G). Scanning EM examination showed in a complementary way that the vasculature in these tumors was lined by cells that resembled endothelial cells (Figure 7A) and that blood lakes were bordered by tumor cells (Figure 7, B and C).

The defective lining layer of tumor vessels was further investigated by examining MCa-IV tumors by transmission EM. Two or more incomplete layers of lining cells were evident in many vessels (Figure 7D). Lining cells in contact with the vessel lumen were heterogeneous in appearance (Figure 7, D and E) and had many features not found in normal endothelial cells. Some regions of lining cells were tightly apposed and joined by junctions (Figure 7E), whereas others were separated from one another (Figure 7F). The cells varied in thickness from ~0.1 μm in attenuated regions to as much as 4 μm near the nucleus (Figure 7E), and some had irregular finger-like projections (Figure 7G). The lining cells had a normal looking nucleus and cytoplasm rich in rough endoplasmic reticulum and mitochondria, typical of metabolically active rather than apoptotic cells (Figure 7, E and F).

Vessel lining cells had a basement membrane that blended into the extracellular matrix around the stromal cells located between vessels and tumor cells (Figure 7, F and G). Tumor cell clusters were also bordered by basement membrane. When multiple layers of flattened cells were located between the vessel lumen and tumor cells, vessel lining cells were not readily distinguished from pericytes or stromal cells (Figure 7G). The basement membrane-like extracellular matrix, which consisted in some regions of multiple layers and in others of a solid matrix (Figure 7, D, F, and G), contributed to the difficulty in distinguishing endothelial cells, pericytes, stromal cells, and tumor cells by transmission EM.

Intercellular Openings

Round or oval openings were present between lining cells of many vessels in MCa-IV tumors examined by scanning EM (Figure 8, A–C). Diameters calculated from the areas of 100 openings in 5 tumors averaged 1.7 ± 0.2 μm (mean ± SE; range, 0.3–4.7 μm). These values were conservative estimates because they tended to minimize the pore size. The size was skewed slightly toward smaller openings, with a median of 1.5 μm (Figure 9). Diameter estimates from perimeters (2.2 ± 0.2 μm; range, 0.3–5.4 μm) gave the maximum diameter openings could achieve, regardless of their shape. Intercellular openings were visible between 29% of the cells, assuming 100 openings among the 700 cells examined and the involvement of two cells per opening. These openings constituted approximately 0.1% of the luminal surface examined (292 μm^2 of 291,000 μm^2). Basement membrane was visible through five of the openings (Figure 8A); the remainder appeared dark by scanning EM, and the underlying structures could not be identified. Narrow slit-like spaces, similar to the oblique slits that form between endothelial cells of inflamed vessels,[48] were found between many cells, but the size and patency of these pathways were difficult to judge; therefore, they were excluded from the measurements. Openings in the lining layer were also evident by transmission EM (Figure 8D).

Figure 6. Blood lakes in pancreatic islet cell tumors in transgenic RIP-Tag2 mice. Brightfield (**A**) and fluorescence (**B**) micrographs showing blood lakes (**arrows**) in a whole mount of a small (~1 mm) RIP-Tag2 tumor. In **A**, red blood lakes stand out from the remainder of the tumor washed free of blood by vascular perfusion of fixative. In **B**, blood lakes appear black, whereas blood vessels are marked by green fluorescent lectin and orange-red fluorescent cationic liposomes injected intravenously before fixation. Cationic liposome fluorescence predominates in the tumor; lectin fluorescence predominates in the surrounding normal acinar pancreas. **C:** Histological section of RIP-Tag tumor showing blood lakes. Also shown are tumor vessels (*), which are much smaller than the lakes and were emptied of blood by perfusion of fixative. Hematoxylin-and-eosin-stained 2-μm methacrylate section. **D** and **E:** Transmission EM of blood lakes showing erythrocytes (RBC) next to tumor cells. **D** illustrates the proximity of RBC and tumors (**arrowheads**). **F** and **G:** Transmission EM showing endothelial cells (**arrows**) of tumor blood vessels, emptied of blood by perfusion fixation, surrounded by extravasated erythrocytes (RBC). In **G**, the blood vessel and cluster of tumor cells are enveloped by multiple layers of basement membrane (**arrowheads**). At this site, an erythrocyte and tumor cells are separated by basement membrane (**apposing arrowheads**). Scale bar in **G** applies to all figures; bar length represents 150 μm in **A** and **B**; 30 μm in **C**; 3 μm in **D** and **F**; 1 μm in **E** and **G**.

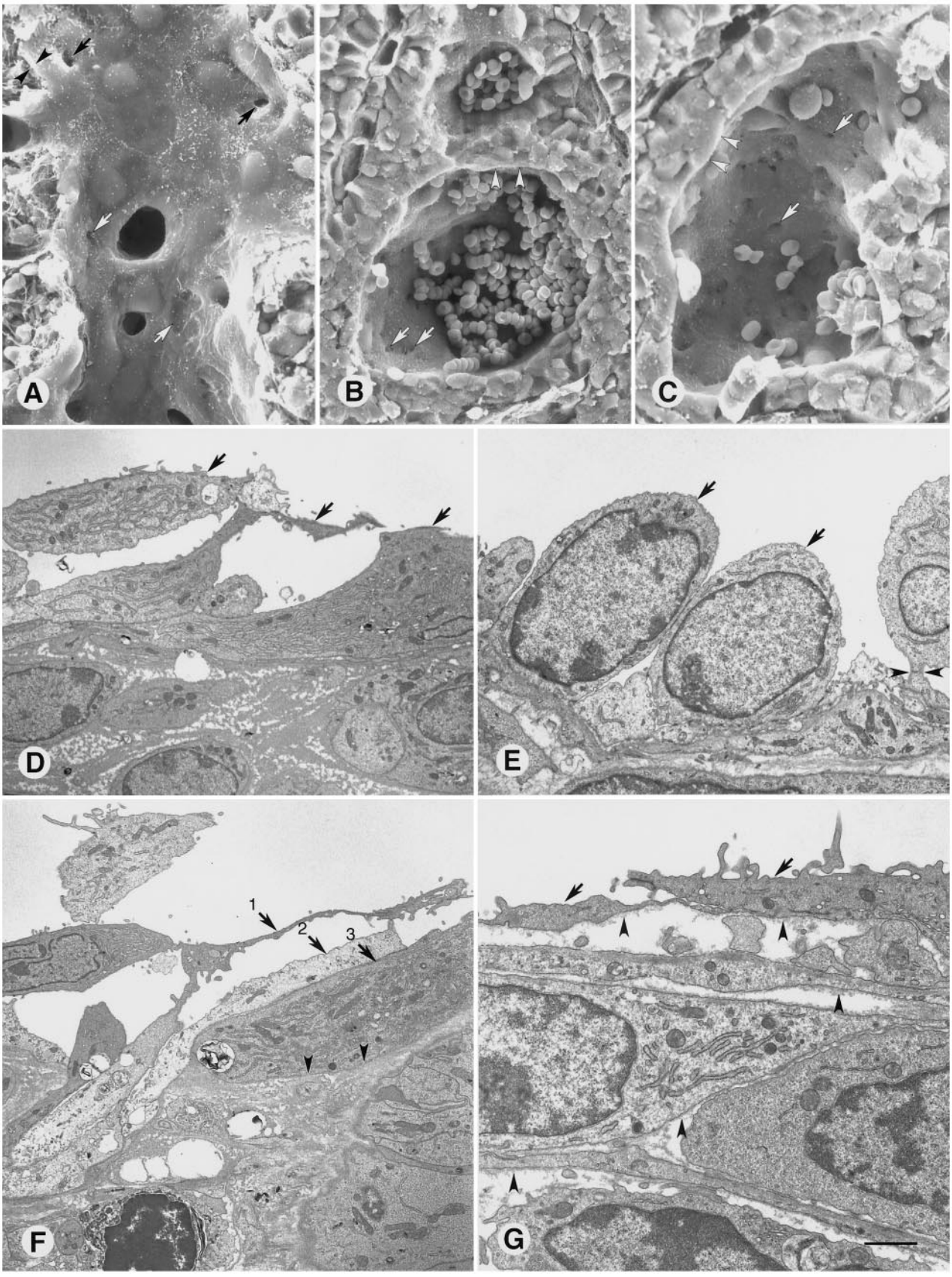
A
B
C
D
E
1
2
3
F
G

Transcellular Holes and Fenestrae

Eight transcellular holes were found along with the 100 intercellular openings in the sample of 700 vessel lining cells in MCa-IV tumors examined by scanning EM (Figure 8, B and C). The diameter calculated from the area of transcellular holes was 0.6 ± 0.1 μm (range, 0.2–0.9 μm; Figure 9). The interior was dark and unidentifiable in seven of the holes, but in one, the plasma membrane of an underlying cell was visible, so it is unclear whether it was a route for extravasation. The eight holes occupied a total area of 2.3 μm^2, which was 0.8% of the area represented by the 100 intercellular openings present in the same sample and 0.0008% of the luminal surface area.

Fenestrae with diaphragms approximately 50 to 80 nm in diameter were visible by transmission EM in thin regions of cells lining MCa-IV tumor vessels (Figure 8E). Clusters of fenestrae were visible by scanning EM (Figure 8F) in 30% of a sample of 55 lining cells; 59% of these fenestrated cells were branched cells.

Discussion

The present study sought to determine the mechanism of tumor vessel leakiness by using complementary light and electron microscopic techniques to examine the vasculature of tumors chosen for their documented vessel leakiness. We found that 14% of the surface area of vessels in MCa-IV mouse mammary carcinomas had a defective endothelial monolayer composed of cells morphologically quite unlike normal endothelial cells. Using immunohistochemistry for cell identification and scanning EM to obtain a high resolution, three-dimensional view of the luminal surface of tumor vessels, we found that all of the lining cells exhibited abnormalities. The cells were immunoreactive for the endothelial cell marker CD31, and some had typical endothelial fenestrae. But most of the cells had an abnormal shape ranging from slightly irregular to multipolar with 50-μm cytoplasmic projections. Some cells overlapped one another and were loosely interconnected. Openings between the cells created 0.3- to 4.7-μm pathways for plasma leakage. In addition to abnormalities visible on the luminal surface, CD31-immunoreactive sprouts radiated from the abluminal surface of some tumor vessels. These findings indicate that both surfaces of the endothelium of tumor vessels are abnormal. Defects in the endothelial monolayer explain the leakiness of the vessels.

Pathways for Plasma Leakage in Tumors

The main goal of this study was to identify the anatomical pathway for extravasation of particles as large as 2 μm from tumor vessels.[30,31] Our scanning and transmission EM observations revealed multiple defects in the lining of MCa-IV tumor vessels and identified three pathways that have been implicated in plasma leakage: openings between the vessel lining cells, holes through the lining cells, and endothelial fenestrae. Of these, intercellular openings are the most likely to explain the unusual leakiness of the MCa-IV tumor vessels. The 1.7 μm average diameter of the intercellular openings corresponds well to the 1.2 to 2.0 μm functional pore cutoff size measured by the extravasation of sterically stabilized (stealth) liposomes in these tumors.[31] The openings were more than 10 times as numerous as transcellular holes, and their combined surface area was over 100 times that of transcellular holes. By comparison, transcellular holes in vessels of MCa-IV tumors had an average diameter of only 0.6 μm.

Data from the present study confirmed the presence of endothelial fenestrae in vessels of MCa-IV tumors.[31] Fenestrae are present in many other tumors as well as in vessels exposed to vascular endothelial growth factor and in some types of normal vessels.[5,52,53] However, endothelial fenestrae are unlikely candidates for the extravasation of 2-μm tracer particles because of their much smaller diameter (~50–80 nm) and diaphragm with channels of < 6 nm diameter.[54]

The morphological data obtained not only match the functional pore size but also fit well with previous evidence of intercellular openings in the vessels of MCa-IV tumors[31] and are consistent with many other reports of open junctions or endothelial gaps, spaces, or discontinuities in tumor vessels.[31,41,52,53,55–57] Further support for the involvement of intercellular openings was the use of multiple complementary methods without particulate tracers that are reported to alter permeability.[58] This evidence does not, however, exclude the participation of pinocytotic vesicles or vesiculo-vacuolar organelles in transvascular transport across tumor vessels.[25,59,60] Indeed, it has been suggested that vesiculo-vacuolar organelles give rise to transendothelial holes.[44,61] The process of macropinocytosis, used by dendritic cells to internalize soluble antigens constitutively,[62] is another possibility, but we are not aware of evidence that this process can translocate 2-μm particles across the endothelial barrier.

Figure 7. A–C: Scanning EM comparison of blood vessel (**A**) and extravascular blood lakes (**B** and **C**) in pancreatic islet cell tumors of transgenic RIP-Tag2 mice. **A:** Tumor vessel, emptied of blood by perfusion of fixative, has a well defined lining layer (**arrowheads**) with scattered defects (**arrows**). **B** and **C:** Blood lakes, which contain extravasated erythrocytes, lined by tumor cells (**arrowheads**). Few of the erythrocytes remain in **C**, showing the tumor surface and multiple holes between the tumor cells (**arrows**). **D–G:** Transmission EM view of abnormal lining cells in MCa-IV tumor vessels. The vessel lumen is at the top of each figure. **D:** Multiple layers of loosely connected cells (**arrows 1–3**) line a tumor vessel. **E:** Tall, rounded cells (**arrows**) with large nuclei, morphologically quite different from those in **D**, form the lining of this tumor vessel. One cell (**arrowhead**) is connected to others by a stalk. **F:** Three lining cells (**arrows 1–3**) are layered on top of one another in the wall of a tumor vessel. Parts of each are in contact with the vessel lumen. The abluminal surface of cell 3 is bordered by dense extracellular matrix (**arrowheads**). **G:** Basement membrane (**arrowheads**) of variable thickness on the abluminal surface of cells (**arrows**) lining a tumor vessel as well as on the surface of multiple cells beneath. Scale bar in **G** applies to all figures; bar length represents 15 μm in **A** and **C**; 20 μm in **B**; 4 μm in **D–F**; 2 μm in **G**.

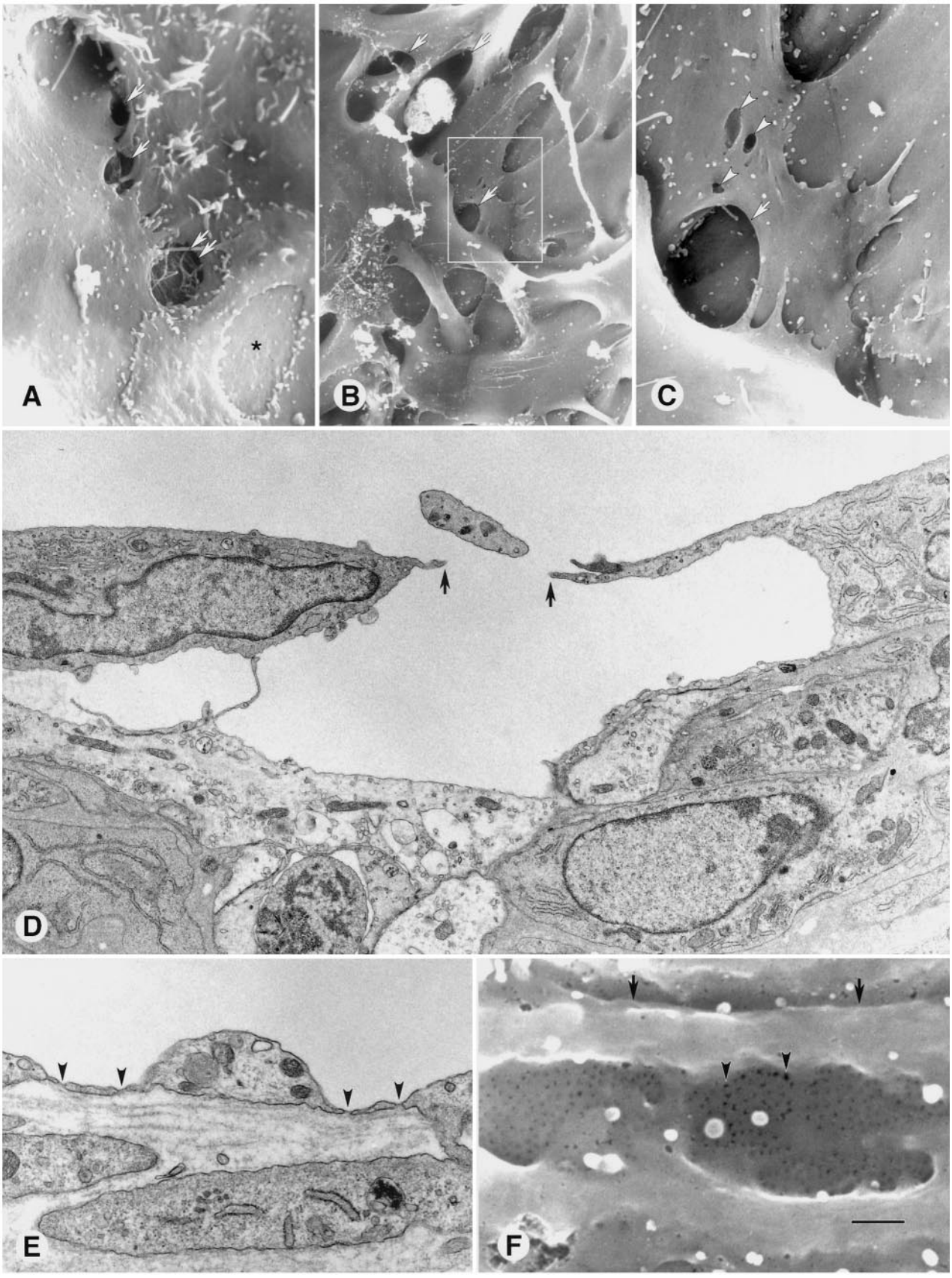
A
B
C
D
E
F

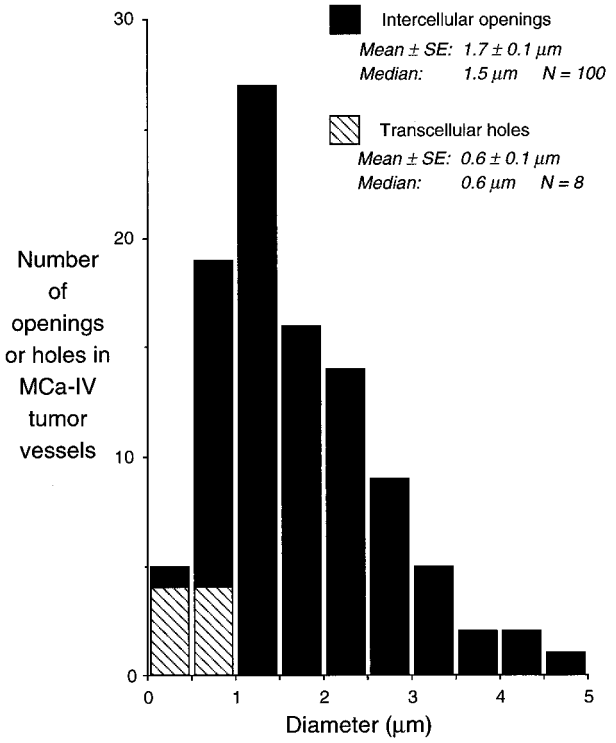

Figure 9. Bar graph showing size distribution of 100 intercellular openings and 8 transcellular holes found in a sample of 700 lining cells in blood vessels of MCa-IV tumors viewed by scanning EM. Diameters were calculated from area measurements of the openings with the assumption that they were circular. Transcellular holes in the sample were treated similarly.

Hemorrhage is another sign of tumor vessel leakiness.[22,35,36,38,63] Many extravasated erythrocytes were present individually and in blood lakes in RIP-Tag2 tumors, but few were present in MCa-IV tumors. Blood lakes were a conspicuous feature of enlarged "angiogenic" islets and tumors in the pancreas of RIP-Tag2 mice and were readily seen with the naked eye, although these red spots have previously been interpreted as angiogenic blood vessels that form at a particular stage of tumorigenesis.[45,46] We found that the blood lakes were lined by tumor cells and did not communicate directly with the vasculature. Our finding that the lakes did not contain cationic liposomes or Monastral blue, which have short half-lives in the bloodstream, suggests that blood lakes form when vessel wall integrity is transiently disrupted. This periodic hemorrhage may be linked to sprouting angiogenesis driven by growth factors that predispose to bleeding.[13,22,64]

The presence of extravasated erythrocytes in tumors has further significance. A recent publication argues that blood vessels of malignant eye tumors known as uveal melanomas are formed by tumor cells instead of endothelial cells.[40] The argument is based in part on ultrastructural evidence of erythrocytes located next to tumor cells, which were presumed to line vascular channels. However, a more likely explanation, suggested by other studies of uveal melanomas[39,65] and the present findings, is that most erythrocytes in contact with tumor cells are not moving through the tumor but rather have left the circulation and are stagnant, at least over the time scale of 30 minutes or so. Studies using long half-life tracers or intravital microscopy may help to determine the time course of extravasation and fate of these cells.

Intercellular Openings versus *Intercellular Gaps in Tumor Vessels*

We used the term intercellular openings to distinguish the large, irregular spaces between branched lining cells of tumor vessels from intercellular gaps that form at endothelial cell borders in inflamed vessels.[43] The intercellular openings of tumor vessels were much larger than the uniform ~0.5-μm intercellular gaps produced by inflammatory mediators.[48,51] Also, the intercellular openings in tumor vessels had no obvious structural features that could result in their closure, unlike rapidly reversible endothelial gaps in inflamed vessels, which are spanned by fingerlike projections that may assist in their closure. Exactly how intercellular openings form in tumor vessels is not understood, although growth factors like vascular endothelial growth factor and angiopoietin-2 may contribute.[13,64] Also, endothelial cells in tumor vessels have a greater motility and more rapid turnover (higher mitotic and apoptotic rates) than normal endothelial cells.[66–71] As a result, intercellular junctions and extracellular matrix attachments may not form normally, leading to impaired monolayer formation and barrier function.

Identity of Lining Cells in Tumor Vessels

In the present study, we have cautiously referred to the lining cells of tumor vessels, rather than assuming that these cells are endothelial cells. Blood vessels in MCa-IV tumors were lined by a distinct layer of CD31-immunoreactive cells and some of the cells had fenestrae. Therefore, these cells appeared to be endothelial cells, albeit abnormal. Although no unstained regions were detected, we recognize that it would be difficult to identify scattered CD31-negative cells in our tissue preparations. Also, despite the apparent homogeneity of CD31 staining, the lining cells were obviously morphologically heterogeneous, with unbranched and branched phenotypes, and the presence of other cell types such as tumor cells, pericytes, or stromal cells cannot be excluded.

Figure 8. Potential pathways for leakage from blood vessels in MCa-IV tumors. **A:** Three intercellular openings (**arrows**) between lining cells of a tumor vessel viewed by scanning EM. Basement membrane is visible through the largest opening (**double arrows**). A large hole through one lining cell exposes the plasma membrane of an underlying cell (*). **B** and **C:** Multiple intercellular openings (**arrows**) and three transcellular holes (**arrowheads**) in branched lining cells of a tumor vessel. The intercellular openings are much larger than the holes. Region in box in **B** is shown at higher magnification in **C**. **D:** Intercellular opening (between **arrows**) in lining of a tumor vessel viewed by transmission EM. **E** and **F:** Fenestrae (**arrowheads**) in lining cells of MCa-IV blood vessels as seen by transmission EM (**E**), which reveals the fenestral diaphragms, and scanning EM (**F**), which shows clusters of fenestrae in a thin region of a horizontally oriented cytoplasmic projection (**arrows**). Scale bar in **F** applies to all figures; bar length represents 2.5 μm in **A** and **C**; 10 μm in **B**; 2 μm in **D**; 0.5 μm in **E**; 0.75 μm in **F**.

In some tumors, blood vessels have been reported to have a discontinuous or absent endothelial cell lining, so that blood flows directly past exposed tumor cells.[1,40,52,72] It has also been claimed that tumor cells can be incorporated as structural elements of the vessel wall and contribute to a cellular mosaic of lining cells.[1,73] Even though our results are consistent with abnormal endothelial cells constituting the lining of MCa-IV tumors, our immunohistochemical studies did not provide conclusive information about the other tumors. Definitive identification of the lining cells, particularly the branched phenotype, awaits unambiguous ultrastructural localization with the appropriate cell markers.

There is no consensus on the single best marker of endothelial cells. Immunohistochemical markers, such as von Willebrand factor and P-selectin, and properties such as uptake of acetylated low-density lipoprotein and lectin staining are not uniformly distributed in endothelial cells of the normal microvasculature,[50,74] and their characteristics in abnormal vessels are incompletely understood. For this reason, we labeled tumor blood vessels by several different methods, and analyzed the similarities and differences in the results. CD31-immunoreactive cells in MCa-IV tumors appeared to be restricted to vessel lining cells and sprouts emanating from them, consistent with what has been observed in other tumors.[75] However, some tumor cells have been reported to have CD31 immunoreactivity.[40,76,77]

Like CD31 immunoreactivity, i.v. injected *L. esculentum* lectin identified vessel lining cells in tumors, but the lectin extravasated from some tumor vessels and stained scattered cells in the stroma. Cationic liposomes also labeled the lining cells of tumor vessels and produced a sharper image of tumor vessels than lectin staining because of the limited extravasation.[12] Cationic liposomes intensely labeled all tumor vessels, consistent with our previous observations that it is not just the newly formed vessels in tumors that avidly take up these liposomes. Pre-existing parts of the tumor vasculature behave the same as vessels undergoing remodeling and angiogenesis.[12] This finding is consistent with our scanning EM observations suggesting that the lining cells of tumor vessels are much more dynamic than normal endothelial cells.

Transluminal Processes, Sprouts, and Other Abnormalities of Vessels

Cells with cytoplasmic projections that bridged the vessel lumen are reminiscent of endothelial cells in vessels undergoing intussusceptive growth in which transluminal bridges eventually partition the vessel lumen.[78,79] Our finding that the number of structures with CD31 immunoreactivity exceeded the number of vessels labeled by lectin or cationic liposomes probably reflects the presence of endothelial cell sprouts without lumens that are growing into the tumor[75,80] or regions of intermittent perfusion.[81] These sprouts may be vessel precursors.

Scanning EM provided detailed, informative views of the luminal surface of vessels, but gave little information about the deeper layers of the vascular wall. Observations from lectin staining, CD31 immunohistochemistry, uptake of fluorescent cationic liposomes, and transmission EM confirmed the multilayered nature of the vessel lining and the heterogeneity of the lining cells. Vessels in the tumors examined were not enveloped by layers of normal smooth muscle cells. Further studies will be needed to determine the number and distribution of pericytes in vessel walls and the role of pericytes in permeability defects in tumor vessels.

Clinical Implications of Tumor Vessel Leakiness

The presence of a defective endothelial monolayer with large anatomical pathways for extravasation has important implications for viral and nonviral gene therapy and other macromolecular treatments of cancer that depend on the leakiness of tumor vessels for their efficacy.[82] Also, studies using dynamic magnetic resonance imaging suggest that tumor vessel permeability is correlated with malignancy in an experimental tumor model.[21] The observation that endothelial cells of some vascular sprouts are not in contact with the vessel lumen indicates that blood borne antiangiogenic agents may not have direct access to all endothelial cells in tumors.

Vascular endothelial growth factor and the angiopoietins are critical regulators of the balance between vascular growth, maturation, and regression, and the leakiness associated with the defective endothelial monolayer of tumor vessels.[13] If vessel leakiness is a functional abnormality that helps tumors survive, therapeutic reversal of the leak through agents targeted to endothelial cells may be clinically beneficial.[83]

In conclusion, we have shown that blood vessels in tumors known to be leaky have a defective endothelial monolayer. Although some tumor vessels have relatively normal lining cells, others are lined by branched, overlapping, disorganized, and loosely interconnected cells. Most of the lining cells appear to be abnormal endothelial cells, but the presence of other cell types cannot be excluded. Spaces between the poorly connected, branched lining cells are the most likely candidates for the pathway for extravasation of particles as large as 2 μm from tumor vessels.

Acknowledgments

We thank Douglas Hanahan for providing the RIP-Tag2 transgenic mice and for many helpful discussions, Amy Haskell for performing the transmission electron microscopy, and the Department of Pathology at University of California San Francisco for use of their scanning electron microscope.

References

1. Warren BA: The vascular morphology of tumors. Tumor Blood Circulation: Angiogenesis, Vascular Morphology and Blood Flow of Experimental and Human Tumors. Edited by Peterson H-I. Boca Raton, CRC Press, Inc., 1979, pp 1–48
2. Less JR, Skalak TC, Sevick EM, Jain RK: Microvascular architecture

in a mammary carcinoma: branching patterns and vessel dimensions. Cancer Res 1991, 51:265–273
3. Konerding MA, Miodonski AJ, Lametschwandtner A: Microvascular corrosion casting in the study of tumor vascularity: a review. Scanning Microsc 1995, 9:1233–1243 (discussion, Scanning Microsc 1995, 9:1243–1244)
4. Less JR, Posner MC, Skalak TC, Wolmark N, Jain RK: Geometric resistance and microvascular network architecture of human colorectal carcinoma. Microcirculation 1997, 4:25–33
5. Papadimitrou JM, Woods AE: Structural and functional characteristics of the microcirculation in neoplasms. J Pathol 1975, 116:65–72
6. Steinberg F, Konerding MA, Streffer C: The vascular architecture of human xenotransplanted tumors: histological, morphometrical, and ultrastructural studies. J Cancer Res Clin Oncol 1990, 116:517–524
7. Vermeulen PB, Verhoeven D, Fierens H, Hubens G, Goovaerts G, Van Marck E, De Bruijn EA, Van Oosterom AT, Dirix LY: Microvessel quantification in primary colorectal carcinoma: an immunohistochemical study. Br J Cancer 1995, 71:340–343
8. Hewitt RE, Powe DG, Morrell K, Balley E, Leach IH, Ellis IO, Turner DR: Laminin and collagen IV subunit distribution in normal and neoplastic tissues of colorectum and breast. Br J Cancer 1997, 75:221–229
9. Dvorak HF, Detmar M, Claffey KP, Nagy JA, van de Water L, Senger DR: Vascular permeability factor/vascular endothelial growth factor: an important mediator of angiogenesis in malignancy and inflammation. Int Arch Allergy Immunol 1995, 107:233–235
10. Friedlander M, Brooks PC, Shaffer RW, Kincaid CM, Varner JA, Cheresh DA: Definition of two angiogenic pathways by distinct alpha v integrins. Science 1995, 270:1500–1502
11. Risau W: Mechanisms of angiogenesis. Nature 1997, 386:671–674
12. Thurston G, McLean JW, Rizen M, Baluk P, Haskell A, Murphy TJ, Hanahan D, McDonald DM: Cationic liposomes target angiogenic endothelial cells in tumors and chronic inflammation in mice. J Clin Invest 1998, 101:1401–1413
13. Holash J, Maisonpierre PC, Compton D, Boland P, Alexander CR, Zagzag D, Yancopoulos GD, Wiegand SJ: Vessel cooption, regression, and growth in tumors mediated by angiopoietins and VEGF. Science 1999, 284:1994–1998
14. Valtola R, Salven P, Heikkila P, Taipale J, Joensuu H, Rehn M, Pihlajaniemi T, Weich H, deWaal R, Alitalo K: VEGFR-3 and its ligand VEGF-C are associated with angiogenesis in breast cancer. Am J Pathol 1999, 154:1381–1390
15. Peterson HI, Appelgren L: Tumour vessel permeability and transcapillary exchange of large molecules of different size. Bibl Anat 1977, 15:262–265
16. Peterson H-I: Vascular and extravascular spaces in tumors: tumor vascular permeability. Tumor Blood Circulation: Angiogenesis, Vascular Morphology and Blood Flow of Experimental and Human Tumors. Edited by Peterson H-I. Boca Raton, CRC Press, Inc., 1979, pp 77–85
17. Gerlowski LE, Jain RK: Microvascular permeability of normal and neoplastic tissues. Microvasc Res 1986, 31:288–305
18. Jain RK: Transport of molecules across tumor vasculature. Cancer Metastasis Rev 1987, 6:559–593
19. Dvorak HF, Nagy JA, Dvorak JT, Dvorak AM: Identification and characterization of the blood vessels of solid tumors that are leaky to circulating macromolecules. Am J Pathol 1988, 133:95–109
20. Jain RK: The Eugene M. Landis Award Lecture 1996: Delivery of molecular and cellular medicine to solid tumors. Microcirculation 1997, 4:1–23
21. Daldrup H, Shames DM, Wendland M, Okuhata Y, Link TM, Rosenau W, Lu Y, Brasch RC: Correlation of dynamic contrast-enhanced MR imaging with histologic tumor grade: comparison of macromolecular and small-molecular contrast media. Am J Roentgenol 1998, 171: 941–949
22. Van den Brenk HA, Crowe M, Kelly H, Stone MG: The significance of free blood in liquid and solid tumours. Br J Exp Pathol 1977, 58: 147–159
23. Liotta LA: Cancer cell invasion and metastasis. Sci Am 1992, 266: 54–59, 62–53
24. Ellis LM, Fidler IJ: Angiogenesis and metastasis. Eur J Cancer 1996, 32A:2451–2460
25. Kohn S, Nagy JA, Dvorak HF, Dvorak AM: Pathways of macromolecular tracer transport across venules and small veins: structural basis for the hyperpermeability of tumor blood vessels. Lab Invest 1992, 67:596–607
26. Nagy JA, Masse EM, Herzberg KT, Meyers MS, Yeo KT, Yeo TK, Sioussat TM, Dvorak HF: Pathogenesis of ascites tumor growth: vascular permeability factor, vascular hyperpermeability, and ascites fluid accumulation. Cancer Res 1995, 55:360–368
27. Lichtenbeld HC, Yuan F, Michel CC, Jain RK: Perfusion of single tumor microvessels: application to vascular permeability measurement. Microcirculation 1996, 3:349–357
28. Dvorak HF, Nagy JA, Feng D, Brown LF, Dvorak AM: Vascular permeability factor/vascular endothelial growth factor and the significance of microvascular hyperpermeability in angiogenesis. Curr Top Microbiol Immunol 1999, 237:97–132
29. Leunig M, Yuan F, Menger MD, Boucher Y, Goetz AE, Messmer K, Jain RK: Angiogenesis, microvascular architecture, microhemodynamics, and interstitial fluid pressure during early growth of human adenocarcinoma LS174T in SCID mice. Cancer Res 1992, 52:6553–6560
30. Yuan F, Dellian M, Fukumura D, Leunig M, Berk DA, Torchilin VP, Jain RK: Vascular permeability in a human tumor xenograft: molecular size dependence and cutoff size. Cancer Res 1995, 55:3752–3756
31. Hobbs SK, Monsky WL, Yuan F, Roberts WG, Griffith L, Torchilin VP, Jain RK: Regulation of transport pathways in tumor vessels: role of tumor type and microenvironment. Proc Natl Acad Sci USA 1998, 95:4607–4612
32. Kaidoh T, Yasugi T, Uehara Y: The microvasculature of the 7,12-dimethylbenz(a)anthracene (DMBA)- induced rat mammary tumour. I. Vascular patterns as visualized by scanning electron microscopy of corrosion casts. Virchows Arch A Pathol Anat Histopathol 1991, 418: 111–117
33. Schwickert HC, Stiskal M, Roberts TP, van Dijke CF, Mann J, Muhler A, Shames DM, Demsar F, Disston A, Brasch RC: Contrast-enhanced MR imaging assessment of tumor capillary permeability: effect of irradiation on delivery of chemotherapy. Radiology 1996, 198:893–898
34. Pham CD, Roberts TP, van Bruggen N, Melnyk O, Mann J, Ferrara N, Cohen RL, Brasch RC: Magnetic resonance imaging detects suppression of tumor vascular permeability after administration of antibody to vascular endothelial growth factor. Cancer Invest 1998, 16: 225–230
35. Schechter JE, Felicio LS, Nelson JF, Finch CE: Pituitary tumorigenesis in aging female C57BL/6J mice: a light and electron microscopic study. Anat Rec 1981, 199:423–432
36. Liwnicz BH, Wu SZ, Tew JM Jr: The relationship between the capillary structure and hemorrhage in gliomas. J Neurosurg 1987, 66:536–541
37. Schechter J, Ahmad N, Elias K, Weiner R: Estrogen-induced tumors: changes in the vasculature in two strains of rat. Am J Anat 1987, 179:315–323
38. Meis-Kindblom JM, Kindblom LG: Angiosarcoma of soft tissue: a study of 80 cases. Am J Surg Pathol 1998, 22:683–697
39. Duke-Elder S, Perkins ES: Cysts and tumours of the uveal tract. System of Ophthalmology, chapter VI. Edited by Duke-Elder S. St. Louis, CV Mosby Company, 1966, pp 754–937
40. Maniotis AJ, Folberg R, Hess A, Seftor EA, Gardner LM, Pe'er J, Trent JM, Meltzer PS, Hendrix MJ: Vascular channel formation by human melanoma cells in vivo and in vitro: vasculogenic mimicry. Am J Pathol 1999, 155:739–752
41. Roberts WG, Delaat J, Nagane M, Huang S, Cavenee WK, Palade GE: Host microvasculature influence on tumor vascular morphology and endothelial gene expression. Am J Pathol 1998, 153:1239–1248
42. Majno G, Palade GE: Studies on inflammation. 1. The effect of histamine and serotonin on vascular permeability: an electron microscopic study. J Biophys Biochem Cytol 1961, 11:571–605
43. McDonald DM, Thurston G, Baluk P: Endothelial gaps as sites for plasma leakage in inflammation. Microcirculation 1999, 6:7–22
44. Michel CC, Neal CR: Openings through endothelial cells associated with increased microvascular permeability. Microcirculation 1999, 6:45–54
45. Hanahan D: Transgenic mice as probes into complex systems. Science 1989, 246:1265–1275
46. Parangi S, Dietrich W, Christofori G, Lander ES, Hanahan D: Tumor suppressor loci on mouse chromosomes 9 and 16 are lost at distinct stages of tumorigenesis in a transgenic model of islet cell carcinoma. Cancer Res 1995, 55:6071–6076

47. Hanahan D: Heritable formation of pancreatic beta-cell tumours in transgenic mice expressing recombinant insulin/simian virus 40 oncogenes. Nature 1985, 315:115–122
48. Baluk P, Hirata A, Thurston G, Fujiwara T, Neal CR, Michel CC, McDonald DM: Endothelial gaps: time course of formation and closure in inflamed venules of rats. Am J Physiol 1997, 272:L155–L170
49. Thurston G, Baluk P, Hirata A, McDonald DM: Permeability-related changes revealed at endothelial cell borders in inflamed venules by lectin binding. Am J Physiol 1996, 271:H2547–H2562
50. McLean JW, Fox EA, Baluk P, Bolton PB, Haskell A, Pearlman P, Thurston G, Umemoto EY, McDonald DM: Organ-specific endothelial cell uptake of cationic liposome-DNA complexes in mice. Am J Physiol 1997, 273:H387–H404
51. McDonald DM: Endothelial gaps and permeability of venules in rat tracheas exposed to inflammatory stimuli. Am J Physiol 1994, 266: L61–L83
52. Sato T, Takusagawa K, Asoo N, Ariji F, Shida K, Kumano N, Konno K: Ultrastructure of the Lewis lung carcinoma. Eur J Cancer Clin Oncol 1982, 18:369–376
53. Roberts WG, Palade GE: Neovasculature induced by vascular endothelial growth factor is fenestrated. Cancer Res 1997, 57:765–772
54. Bearer EL, Orci L: Endothelial fenestral diaphragms: a quick-freeze, deep-etch study. J Cell Biol 1985, 100:418–428
55. Toth B, Malick L: Scanning electron-microscopic study of the surface characteristics of neoplastic endothelial cells of blood vessels. J Pathol 1976, 118:59–63
56. Hamazaki M, Tanaka T: Hemangiosarcoma of the breast: case report with scanning electron microscopic study. Acta Pathol Jpn 1978, 28:605–613
57. Endrich B, Hammersen F, Gotz A, Messmer K: Microcirculatory blood flow, capillary morphology and local oxygen pressure of the hamster amelanotic melanoma A-Mel-3. J Natl Cancer Inst 1982, 68:475–485
58. Feng D, Nagy JA, Hipp J, Pyne K, Dvorak HF, Dvorak AM: Reinterpretation of endothelial cell gaps induced by vasoactive mediators in guinea-pig, mouse and rat: many are transcellular pores. J Physiol (Lond) 1997, 504:747–761
59. Cox DJ, Pilkington GJ, Lantos PL: The fine structure of blood vessels in ethylnitrosourea-induced tumours of the rat nervous system: with special reference to the breakdown of the blood-brain barrier. Br J Exp Pathol 1976, 57:419–430
60. Dvorak AM, Kohn S, Morgan ES, Fox P, Nagy JA, Dvorak HF: The vesiculo-vacuolar organelle (VVO): a distinct endothelial cell structure that provides a transcellular pathway for macromolecular extravasation. J Leukoc Biol 1996, 59:100–115
61. Bates DO, Lodwick D, Williams B: Vascular endothelial growth factor and microvascular permeability. Microcirculation 1999, 6:83–96
62. Sallusto F, Cella M, Danieli C, Lanzavecchia A: Dendritic cells use macropinocytosis and the mannose receptor to concentrate macromolecules in the major histocompatibility complex class II compartment: downregulation by cytokines and bacterial products. J Exp Med 1995, 182:389–400
63. Schechter J: Ultrastructural changes in the capillary bed of human pituitary tumors. Am J Pathol 1972, 67:109–126
64. Cheng SY, Nagane M, Huang HS, Cavenee WK: Intracerebral tumor-associated hemorrhage caused by overexpression of the vascular endothelial growth factor isoforms VEGF121 and VEGF165 but not VEGF189. Proc Natl Acad Sci USA 1997, 94:12081–12087
65. Specht CS, McLean IW, Biscoe BW: Traumatic enucleation for posterior uveal melanoma. Am J Ophthalmol 1990, 110:518–521
66. Cavallo T, Sade R, Folkman J, Cotran RS: Tumor angiogenesis: rapid induction of endothelial mitoses demonstrated by autoradiography. J Cell Biol 1972, 54:408–420
67. Warren BA, Greenblatt M, Kommineni VR: Tumour angiogenesis: ultrastructure of endothelial cells in mitosis. Br J Exp Pathol 1972, 53:216–224
68. Ausprunk DH, Folkman J: Migration and proliferation of endothelial cells in preformed and newly formed blood vessels during tumor angiogenesis. Microvasc Res 1977, 14:53–65
69. O'Reilly MS, Boehm T, Shing Y, Fukai N, Vasios G, Lane WS, Flynn E, Birkhead JR, Olsen BR, Folkman J: Endostatin: an endogenous inhibitor of angiogenesis and tumor growth. Cell 1997, 88:277–285
70. Bergers G, Hanahan D, Coussens LM: Angiogenesis and apoptosis are cellular parameters of neoplastic progression in transgenic mouse models of tumorigenesis. Int J Dev Biol 1998, 42:995–1002
71. Jain RK, Safabakhsh N, Sckell A, Chen Y, Jiang P, Benjamin L, Yuan F, Keshet E: Endothelial cell death, angiogenesis, and microvascular function after castration in an androgen-dependent tumor: role of vascular endothelial growth factor. Proc Natl Acad Sci USA 1998, 95:10820–10825
72. Konerding MA, Steinberg F, Budach V: The vascular system of xenotransplanted tumors–scanning electron and light microscopic studies. Scanning Microsc 1989, 3:327–335 (discussion, Scanning Microsc 1989, 3:335–336)
73. Hammersen F, Endrich B, Messmer K: The fine structure of tumor blood vessels. I. Participation of non-endothelial cells in tumor angiogenesis. Int J Microcirc Clin Exp 1985, 4:31–43
74. Thurston G, Baluk P, McDonald DM: Determinants of endothelial cell phenotype in venules. Microcirculation 2000, 7:67–80
75. Berger R, Albelda SM, Berd D, Ioffreda M, Whitaker D, Murphy GF: Expression of platelet-endothelial cell adhesion molecule-1 (PECAM-1) during melanoma-induced angiogenesis in vivo. J Cutan Pathol 1993, 20:399–406
76. Tang DG, Chen YQ, Newman PJ, Shi L, Gao X, Diglio CA, Honn KV: Identification of PECAM-1 in solid tumor cells and its potential involvement in tumor cell adhesion to endothelium. J Biol Chem 1993, 268:22883–22894
77. Aroca F, Renaud W, Bartoli C, Bouvier-Labit C, Figarella-Branger D: Expression of PECAM-1/CD31 isoforms in human brain gliomas. J Neurooncol 1999, 43:19–25
78. Nagy JA, Morgan ES, Herzberg KT, Manseau EJ, Dvorak AM, Dvorak HF: Pathogenesis of ascites tumor growth: angiogenesis, vascular remodeling, and stroma formation in the peritoneal lining. Cancer Res 1995, 55:376–385
79. Patan S, Munn LL, Jain RK: Intussusceptive microvascular growth in a human colon adenocarcinoma xenograft: a novel mechanism of tumor angiogenesis. Microvasc Res 1996, 51:260–272
80. Debbage PL, Griebel J, Ried M, Gneiting T, DeVries A, Hutzler P: Lectin intravital perfusion studies in tumor-bearing mice: micrometer-resolution, wide-area mapping of microvascular labeling, distinguishing efficiently and inefficiently perfused microregions in the tumor. J Histochem Cytochem 1998, 46:627–639
81. Trotter MJ, Chaplin DJ, Durand RE, Olive PL: The use of fluorescent probes to identify regions of transient perfusion in murine tumors. Int J Radiat Oncol Biol Phys 1989, 16:931–934
82. Jain RK: The next frontier of molecular medicine: delivery of therapeutics. Nat Med 1998, 4:655–657
83. Thurston G, Suri C, Smith K, McClain J, Sato TN, Yancopoulos GD, McDonald DM: Leakage-resistant blood vessels in mice transgenically overexpressing angiopoietin-1. Science 1999, 286:2511–2514